Electric Power Systems Research 143 (2017) 14–24

Contents lists available at ScienceDirect

Electric Power Systems Research

journal homepage: www.elsevier.com/locate/epsr

A novel methodology for modeling waveforms for power quality disturbance analysis

Marco A. Rodriguez-Guerrero [a,b], Rene Carranza-Lopez-Padilla [a], Roque A. Osornio-Rios [b], Rene de J. Romero-Troncoso [c,*]

[a] Centro Nacional de Metrología, Carretera a Los Cués km 4.5, 76246, El Marqués, Querétaro, Mexico
[b] HSPdigital – CA Mecatronica, Facultad de Ingenieria Campus San Juan del Rio, Universidad Autonoma de Queretaro, Rio Moctezuma 249, 76807 San Juan del Rio, Queretaro, Mexico
[c] HSPdigital – CA Telematica, DICIS, Universidad de Guanajuato, Carr. Salamanca-Valle km 3.5+1.8, Palo Blanco, 36885 Salamanca, Guanajuato, Mexico

ARTICLE INFO

Article history:
Received 18 March 2016
Received in revised form 8 August 2016
Accepted 6 September 2016

Keywords:
Power quality disturbances
Power quality analysis
Power quality modeling
Parametric mathematical model

ABSTRACT

Nowadays, power quality (PQ) analysis is having more relevance in the operation of power systems due to the increase of power quality events and disturbances. Those disturbances are related to the interconnection of renewable energy generators, and to the highly non-linear characteristics of the load, among others. There is a need of having knowledge about the nature of the PQ disturbances and about the mathematical approaches that describe the PQ disturbance. This paper presents the development of a structured methodology in combination with a mathematical model, intended for describing waveforms that contain simultaneous PQ disturbances. The validation process is made by fitting the proposed model to standard reference waveforms along with field recorded waveforms. The proposed mathematical model is capable of being adjusted in order to reproduce waveforms that contain simultaneous PQ disturbances. Five study cases are presented in order to test the proposed methodology.

1. Introduction

During the last decades, power quality (PQ) analysis on power systems has significantly increased due to its relevance for operational issues like power system stability and propagation of PQ related effects in the grid. It is especially relevant when utilities want to preserve both the quality and the stability in the supply of electric energy, having special interest in the development of novel methods for accurately measuring the value of some power quality indexes (PQI) [1–3]. Typically, for almost every methodology in topics related to PQ analysis such as: detecting, classifying, monitoring or measuring power quality disturbances (PQD), it has been necessary to develop mathematical models for analyzing specific disturbances [4–8]. Those models can be abstracted as mathematical representations of a limited number of disturbances or PQ phenomena in a single event; in that sense, it could be said that the models are partial solutions for particular research problems and they are based on the nature of a specific disturbance, *i.e.* sags [9], swells [10], harmonics [11,12], flickers [13], etc. There are many specific models for several different PQD that allow the simulation or classification of these disturbances on power systems [14]; yet, little has been reported to propose a single, structured and unified mathematical model for a broader description of simultaneous PQ phenomena for different stages on power systems. In other words, only very few approaches combine different phenomena in a single model, solving specific targets in PQ analysis, even when there is evidence that different PQD occurs simultaneously on power systems [15,16]. Most of the proposed models are specific to a single PQD and those that combine some PQD are partial models focused in the specific phenomena of research.

There are approaches developed for classifying or monitoring many PQD [2,3,17,18] by using well-defined mathematical models; however, those models have been designed for partial and particular representations of specific PQD. In the same way, there are standards devoted to PQ matters [4–8], where there can be found definitions, performance tests, benchmarking and even specific mathematical models related to PQ phenomena. These standards are well known in the scientific community and they are widely used in the electric industry. The aim of most PQ standards is to establish the operational limits for voltage stability on power systems in presence of disturbances. Nevertheless, standards do not establish limits for the electric current waveform, mostly because of its high sensitivity to the load, which cannot be generalized, even when the current waveform is typically more distorted than

* Corresponding author.
E-mail address: troncoso@hspdigital.org (R. de J. Romero-Troncoso).

http://dx.doi.org/10.1016/j.epsr.2016.09.003
0378-7796/

the voltage waveform on a given power system. Most analyses are made to comply with the voltage waveform standards, making difficult to truly represent the non-stationary behavior of the current waveform by using specific voltage-related mathematical models. The standards present PQ phenomena models by separating disturbances according to their own nature. These phenomena have been classified in voltage variations (sags and swells), frequency variations, signal distortion (harmonics, inter-harmonics, amplitude modulation, etc.), sensorial perception (flicker), additive noise, high-frequency spurious signals, and transients, among others. Some of these PQD are related to connection and interconnection of renewable generation systems to the main grid, some others are related to non-linear loads that are continuously switching, affecting voltage and current waveforms equally; somehow making measuring, and classifying PQD more complicated [19]. Some reported approaches of PQ analysis have used computational simulations based on mathematical models as a way to represent real waveforms in order to set up algorithms for power quality analysis [20,21]; yet, those approaches are capable of only partially represent PQD, pointing out the need of more detailed models for signal processing. For instance, in [22,23] computational tools for PQ analysis are presented and discussed. In [23] a novel synthetic reference waveform was designed for synchrophasor-related applications; this waveform was designed and coded using a realistic scenario on power systems including harmonic distortion, unbalance, inter-harmonics, oscillatory behavior of voltage amplitude, and modulations in amplitude and phase, among other, but the approach to the mathematical model is not shown, only the temporal description of simultaneous PQD in order to reproduce the testing waveform. Recent approaches [23] show the trend of combining two or more PQD at the same time, being realistic in comparison with a real power system; the abstraction and analysis of two or more simultaneous PQD can be complex, and typically depends on the nature of the PQD and the state of the power system, being necessary to develop a complete organized mathematical model that includes different types of PQD simultaneously.

There is a need to use an organized mathematical model that truly represents those PQD found in real power systems. For instance, in [24] a methodology for generating and validating synthetic waveform for power quality disturbances has been described. Regarding synthetic waveform generation, there are three main methodologies for reproducing electric waveforms in digital ways, using commercial software such as: (1) PSCAD/EMTDC; (2) ATP/EMTP, and (3) Matlab/Simulink. Especially in [24] a methodology based on Matlab/Simulink for simulation of faults on a distribution power system was detailed. The selected disturbances covered five scenarios: voltage amplitude variations, harmonics, interruptions, oscillatory transients and pure sine waveforms. The methodology includes the use of parametric equations and simulation of events in a given power system using Simulink. This work aims at developing computational tools that are more realistic for synthetizing digital waveforms, yet, the mathematical foundations for having a unified model for PQ is not developed and it does not take into account the non-stationary case for waveform generation, being a good research topic for PQ analysis either for synchrophasor dynamic algorithms research or for designing better instruments for detecting, classifying and monitoring PQD in power systems. There are other approaches based on statistical measurements, distribution system modeling and Monte Carlo techniques for PQD simulation [25], but those approaches only approximate PQD in stationary state for non-sinusoidal and unbalanced conditions, this was intended to calculate PQI from a statistical point of view, unlike to develop a reference generator of PQD waveforms.

There is a lack of published works intended for developing PQD analytical models that are capable of representing single disturbances for stationary or non-stationary scenarios, as well as representing the combination of several disturbances occurring simultaneously. It is desirable to have a unified mathematical model, which is capable of representing a wider spectrum of PQD and phenomena, present in the generation, the transmission and the distribution of power systems, accurately. Even more, by using this abstraction it is possible to synthetize accurate digital PQD waveforms for PQ analysis using computational tools.

In this work, a novel methodology for modeling PQD on power systems is presented. It is aimed for improving the mathematical background required in the analysis, classification and synthesis of PQD on power systems. The approach is based on a unified mathematical basis for representing a wider range of disturbances than most models have present to date. Also, it is shown that the development of this particular capability is possible by structuring the model into five main stages; one for modeling the steady-state amplitude-related disturbances including harmonic distortion, a second one for modeling frequency and phase changes of the fundamental frequency and its harmonics, which represents the dynamic behavior of the fundamental frequency. A third one for modeling non-correlated phenomena such as interharmonics; a fourth one for describing transients and finally a section for additive noise with both, Gaussian noise and colored noise. The process for validating the proposed methodology consists in the creation step-by-step of a waveform that contains several simultaneous PQD using the proposed mathematical model and the methodology developed in this work. Additionally, a direct comparison of accuracy against different standard recorded waveforms are carried out; for instance, in the case of waveforms used in working groups in international standards [26], by the use of waveforms stated in international standards [27], by using a set of reference waveforms developed in different National Metrology Institutes (NMI) worldwide [28–30], by using a recorded event in a real power system and finally by reproducing simultaneous non-stationary events and disturbances in a single synthetic waveform. All those scenarios allow comparing the performance of the developed model as a waveform generator; providing an assessment of accuracy and performance for this novel methodology of reproducing simultaneous PQD based on a structured mathematical model. The main potential application is located as an accurate generator for synthetic waveforms (benchmarking) in order to set up and testing signal processing algorithms in PQ analysis, monitoring, classifying, filtering and even for testing synchrophasor algorithms. It is shown that the proposed mathematical tool is capable of adjusting a mathematical model aiming to represent a kind of PQD: when the parameters of a given waveform are known *a priori;* and also when the waveform is obtained from a real recorded sampled signal.

2. Methodology

There are at least three general groups described in the literature to classify PQD by their nature: (a) amplitude phenomena, (b) deviations in the fundamental frequency, and (c) transient events. In general, PQD have been historically classified by their nature, for instance, amplitude phenomena like swells and sags being phenomena that affect directly the amplitude of the system; and frequency deviations or frequency acceleration being phenomena particularly related with stability matters. This classification implies that some efforts have been oriented to achieve solutions either for amplitude issues, or for frequency deviations, or for distorted environments, in an almost exclusive way. Highly specialized algorithms for achieving solutions of measuring, detecting and classifying PQD are commonly set up by the use of mathematical models for reproducing synthetic waveforms in order to stress the methodologies for solving a particular issue in a PQ research

field. Those models are detailed, but they represent just a fraction of all possible PQD in a real power system.

The aim of this work is to provide a methodology for constructing a mathematical tool that can exhibit some key features such as high fidelity of representation of PQ events and capability of representing multiple simultaneous PQD. Some of the advantages of this approach are: (1) the proposed mathematical model covers a wide variety of PQD, being possible to simultaneously represent several PQD; (2) having the proposed model as reference, it is possible to generate synthetized signals that are more representative in order to simulate realistic power system environments and finally; (3) it is possible to tune the mathematical model to obtain a mathematical representation of real waveforms that are recorded by commercial instruments in order to evaluate and validate different methodologies used in the PQ field. There are commercial options available in the market for simulation and generation of waveforms related with PQ events in electric grids; however, those tools are focused on deliver waveforms of a particular PQ event instead of delivering the mathematical behavior of a given waveform. In many cases, for research on PQ topics, a tool for understanding the nature of a PQ event is a key element for PQ analysis. The mathematical tool that is proposed in this work aims to ease the understanding of how a physical event in a grid can be modeled as a well-known structured mathematical model. Even more, the mathematical tool is agile and easy of manipulating in order to generate waveforms that can be used as reference in PQ analysis. This proposed mathematical model is not intended for substituting, competing or replacing any commercial option; furthermore, the proposed mathematical model may be thought as a well-structured complement of those available tools.

The methodology used in this work is based on generating a general parametric mathematical model structured for several PQD into five groups:

1) Phenomena related to the amplitude of the fundamental frequency and harmonics.

Some of the most significant phenomena of PQD are related to the amplitude of the fundamental frequency, including phenomena related to low frequency oscillations in amplitude, amplitude distortions, sags, swells, and interruptions. PQD related to amplitude are directly correlated with faults among lines to ground, by sudden changes in the load, non-linear loads, or unbalanced conditions. These PQD are all correlated to the fundamental frequency and its harmonics. Eq. (1) states the first approximation $x_1(t)$ of the proposed mathematical model for the amplitude-related PQD:

$$x_1(t) = \mathrm{A}\cdot\left[1+\delta(t)\right]\left[\cos\left(2\pi f_0 t+\theta_1\right)+\sum_{h=2}^{N} a_h(t)\cos\left(2\pi h f_0 t+\theta_h\right)\right] \quad (1)$$

where A is the peak value of the amplitude, $\delta(t)$ is a time dependent function that represents events associated to amplitude disturbances such as oscillations, swells, sags and interruptions. The value of the fundamental frequency is f_0, θ_1 is the value of the phase for the fundamental component, whereas t is the independent variable for time. h is the index value of the h-th harmonic up to N. $a_h(t)$ is the time-dependent amplitude factor for the h-th harmonic component correlated to the fundamental and θ_h is the h-th harmonic phase value. For the first approximation model, the fundamental frequency f_0, the phase of the fundamental component, and the phase of each harmonic component θ_h are considered constants.

2) Phenomena related to the fundamental frequency with changes in frequency and phase.

Other significant group of PQD is related to variations in the fundamental frequency and its harmonics. These variations are closely related with stability in power systems, and they are originated by changes in the balance of power flux as well as dynamic changes in the electric characteristics of the load. The PQD associated to fundamental frequency are low-frequency phase modulation, sudden changes in the phase (jumps) and acceleration of the frequency, for instance linear chirps. Eq. (2) represents the second approximation $x_2(t)$ of the proposed mathematical model for time-dependent amplitude, frequency and phase.

$$x_2(t) = A\cdot\left[1+\delta(t)\right]\left\{\cos\left[2\pi f_0(t)\,t+\theta_1(t)\right]+\sum_{h=2}^{N} a_h(t)\cos\left[2\pi h f_0(t)\,t+\theta_h(t)\right]\right\} \quad (2)$$

where A, $\delta(t)$, $a_h(t)$ and t are the same than in Eq. (1). $f_0(t)$ is a time dependent function that represents frequency changes (sinusoidal, square, etc.), $\theta_1(t)$ models phase changes such as low-frequency oscillations, phase jumps, etc.; h is the index value of the h-th harmonic up to N. $\theta_h(t)$ is the h-th harmonic phase value for the h-th harmonic component correlated to the fundamental, which is a time dependent function that is useful for representing dynamic behavior of harmonics. The main difference between Eq. (1) and Eq. (2) is directly related to frequency and phase components in the fundamental and its harmonics. In Eq. (2) the phase and frequency are not constant components, allowing to abstract phenomena such as fluctuant harmonics or non-stationary behavior.

3) Stationary phenomena non-correlated to the fundamental frequency.

Nowadays, the implementation of smart grids, which interconnects renewable energy sources to traditional power systems, is source of PQD that are non-correlated with the fundamental frequency. For instance, the non-linear power electronics devices used in AC-DC inverters generate some additive spurious signals such as high frequency interharmonics, typically frequencies around 1 kHz. Other sources of high frequency components are those related to non-linear loads. Eq. (3) represents the third approximation $x_3(t)$ of the proposed mathematical model for non-correlated components to fundamental frequency.

$$x_3(t) = x_2(t) + \sum_{k=1}^{K} b_k(t)\cos\left[2\pi f_k(t)\,t+\varphi_k(t)\right] \quad (3)$$

where $x_2(t)$ it is the same than Eq. (2). k is the index value of the k-th non-correlated component up to K. $f_k(t)$ is the frequency value of the k-th component that is typically not an exact multiple of the fundamental frequency, $b_k(t)$ is the time-dependent amplitude factor for the k-th component non-correlated to the fundamental and $\varphi_k(t)$ is the time-dependent function regarding to the k-th non-correlated component phase value.

4) Transient phenomena.

PQD of very short duration is typically known as transient phenomena. The transients may be thought as components of high frequency that appear only during a short period; often the transients have a very fast decaying component. The way as the transient decays can be either in combination with oscillatory behavior having a high frequency component or in the presence of a flat noisy notch waveform. Transient phenomena are common during switching conditions when different types of loads are connected or disconnected in a given node in a power system. Transients can be simplified as very fast variations in short periods

defined by two time marks. Eq. (4) includes all the PQD defined above in Eqs. (1)–(3), and adds the short time transients.

$$x_4(t) = x_3(t) + \sum_{m=1}^{M} c_m \left[u(t-\alpha_m) - u\left(t-\beta_m\right)\right] \cdot e\left[\left(-\frac{t-\alpha_m}{\tau_m}\right)\right] \cdot cos\left(2\pi f_m t + \psi_m\right) \quad (4)$$

where t and $x_3(t)$ is the same as Eq. (3). $u(t)$ is the Heaviside step function, α_m defines the time value when the transient starts, β_m defines the time value when the transient ends. m is the index value of the m-th transient up to M. c_m is the amplitude factor for the m-th transient, f_m is the frequency value of the m-th transient, ψ_m is the phase value of the m-th transient. Both, f_m and ψ_m are considered constant in the proposed models. Finally, τ_m is the decay rate value of the transient.

5) Additive random noise, Gaussian and non-Gaussian.

Some additive components cannot be classified as correlated phenomena or as non-correlated phenomena; yet, they are present in electric power systems. For instance, in [14] and [31] situations and events where random behavior affects a power system are depicted. Some events that produce additive noise have been identified, such as starting and operating large arc furnaces, electromagnetic interference or by connecting non-linear loads. Eq. (5) states the fifth approximation $x_5(t)$ of the proposed mathematical model for additive random noise:

$$x_5(t) = x_4(t) + n(t, x_0, \sigma) + \mu(t) \quad (5)$$

Where t and $x_4(t)$ is the same that Eq. (4). The random phenomena is classified and abstracted in two time-dependent functions, first $\eta(t,x_0,\sigma)$ that represents the random Gaussian additive noise, defined with a mean value x_0, and a standard deviation, σ. On the other hand, $\mu(t)$ is the term associated to colored additive noise or additive components with a probability function different from the Gaussian.

2.1. Construction of the proposed mathematical model for PQD

The complete mathematical model proposed in this work is shown in Eq. (6), which is able to depict a combination of several PQD. Based on the proposed model it is possible to synthetize waveforms that are similar, from a mathematical viewpoint, to those recorded in real power systems. Eq. (6) has been constructed adding consecutively from Eq. (1) up to Eq. (5) plus a DC term, X_{DC}; modeled as a constant value and superimposed to the other terms. Eq. (6) summarizes a wide number of different PQD, allowing reproducing waveforms, synthetically, which can be used as reference for PQ analysis.

Another feature of this methodology is that it is possible to program a kind of PQ event to appear in the waveform at a given time, indexing several PQD. In the traditional approach it is common to find parametric solutions, but in a single and separated way. With the proposed methodology, it is also possible to generate accurate benchmarking digital signals for several applications related to PQ issues.

$$x(t) = X_{DC} + A\cdot\left[1+\delta(t)\right]\left\{\cos\left[2\pi f_0(t)t + \theta_1(t)\right] + \sum_{h=2}^{N} a_h(t)\cos\left[2\pi f_0(t)t + \theta_1(t)\right]\right\} + \sum_{k=1}^{K} b_k(t)\cos\left[2\pi f_k(t)t + \varphi_k(t)\right] + \sum_{m=1}^{M} c_m\left[u(t-\alpha_m) - u\left(t-\beta_m\right)\right]\cdot e\left[\left(\frac{t-\alpha_m}{\tau_m}\right)\right]\cdot\cos\left(2\pi f_m t + \psi_m\right) + n(t, x_0, \sigma) + \mu(t) \quad (6)$$

The model of Eq. (6) is one of the most complete to date regarding PQ analysis. The model is not intended to cover all PQD present in a real power system; the field is still open for adding other kind of events, the only requirement it is that these events can be model in a parametric equation.

3. Model validation

This section presents the construction of a synthetic waveform using the model from Eq. (6) in order to validate the proposed methodology and also to show the procedure for generating the desired PQD in the model. The proposed methodology stated in Section 2 is capable of reproducing a wide range of different PQD, and the developed example shows how a waveform is constructed using the methodology. The methodology starts by defining a basis fundamental signal where the PQD are incorporated sequentially. Once the fundamental waveform is defined, the methodology is applied in five steps. During each step, some PQD are added to the waveform in concordance with Eqs. (1)–(6) as follows: (1) In the first step three harmonics are added; (2) in the second step, amplitude disturbances are added, specifically a sag event and a swell event; (3) at the third step, three non-correlated interharmonics are added; (4) in the fourth step, an oscillatory transient is aggregated; (5) and finally, in the fifth step, Gaussian noise is added.

In this example, the fundamental signal used as basis is a pure sinusoidal waveform as stated in Eq. (7)

$$x_a(t) = A\cdot\cos\left[2\pi f_0 t + \theta\right] \quad (7)$$

where $x_a(t)$ stands a single tone resulting waveform; A represents the amplitude of the waveform, f_0 is the constant fundamental frequency value, and θ is the value of the phase given in rads. The independent time variable is expressed with the t variable. At this point of the methodology, the amplitude A and the phase θ are constants. The values used in this example are: $A = 1.0$, $f_0 = 60$ Hz, and $\theta = 0.0$ rads.

At the first step of the methodology, it is added harmonic distortion to the fundamental signal $x_a(t)$ in equation Eq. (7), resulting the analytical expression of Eq. (8)

$$x_b(t) = x_a(t) + \sum_{h=2}^{N} a_h \cos\left[2\pi h f_0 t + \theta_h\right] \quad (8)$$

where $x_b(t)$ stands a fundamental frequency waveform with harmonic distortion; h is the index related with the h-th harmonic value, N is the value of the higher order harmonic; a_h represents de values of amplitude of each harmonic, θ_h represents the values of phase of each harmonic, and f_0 is the constant fundamental frequency value.

For the present example, only three harmonics are chosen. The harmonic distortion contains values for at the 3rd, 5th, and 7th harmonics of the fundamental. The numerical values for the harmonic components are: $N = 7$; $a_2 = a_4 = a_6 = 0$; $a_3 = 0.05$; $a_5 = 0.1$; $a_7 = 0.05$; $\theta_3 = 0.7853$ rads; $\theta_5 = 1.5708$ rads; $\theta_7 = -0.7853$ rads. For even harmonics a zero rads value is assigned. The Fig. 1 shows the resulting waveform $x_b(t)$.

The second step is related to the amplitude phenomena. Two amplitude disturbances events are added to the $x_b(t)$ waveform; a sag event, and a swell event. The analytical expression that represents this addition is stated in Eq. (9).

$$x_c(t) = x_b(t)\cdot\left[1+\delta(t)\right] \quad (9)$$

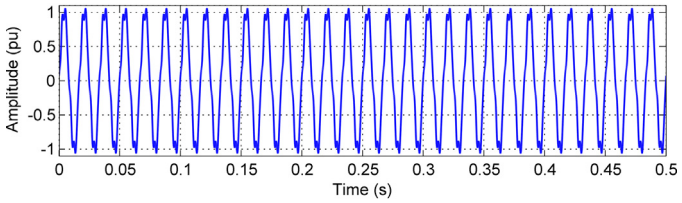

Fig. 1. First step of the construction of a signal with several PQD: fundamental signal at 60 Hz plus harmonic distortion at the 3rd, 5th, and 7th harmonics, $x_b(t)$.

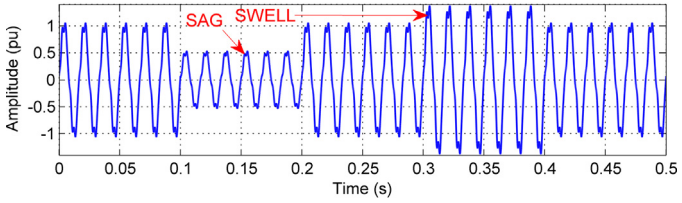

Fig. 2. Second step of the construction of a signal with several amplitude-related PQD are added in the form of a Sag and a Swell.

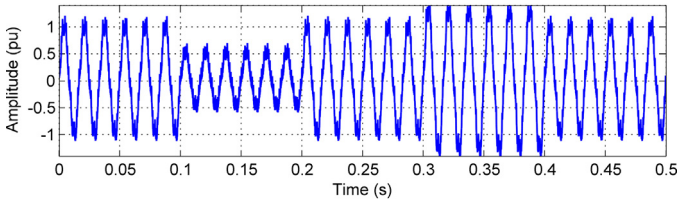

Fig. 3. Third step of the construction of a synthetic signal with several PQD: Appending non-correlated interharmonic distortion, $x_d(t)$.

where $\delta(t)$ represents the changes in the amplitude of the waveform. Eq. (10) shows the behavior of the amplitude during the construction of the waveform $x_c(t)$.

$$\delta(t) = -A_{sag} \cdot \left[u\left(t-\alpha_{sag}\right) + u\left(t-\beta_{sag}\right)\right] + A_{swell} \cdot \left[u(t-\alpha_{swell}) + u\left(t-\beta_{swell}\right)\right] \quad (10)$$

where A_{sag} is the reduction of the amplitude in the resulting waveform due to a sag event. A_{swell} is the increment of the amplitude in the resulting waveform due to a swell event. α_{sag} represents the initial time of the sag event, β_{sag} represents the final time mark of the sag event. For the swell event, α_{swell} stands for the initial time, and β_{swell} is final time mark.

The numerical values for this experiment are: $A_{sag} = 0.5$; $A_{swell} = 0.3$; $\alpha_{sag} = 0.1$ s; $\beta_{sag} = 0.2$ s; $\alpha_{swell} = 0.3$ s $\beta_{swell} = 0.4$ s. Fig. 2 shows the resulting waveform $x_c(t)$ for the second step.

The third step includes phenomena that are non-correlated to the fundamental frequency, such as interharmonic distortion. This interharmonic distortion is added to the resulting waveform of the latter step, $x_c(t)$. The analytical expression for this step is addressed in Eq. (11)

$$x_d(t) = x_c(t) + \sum_{k=1}^{K} b_k \cos\left[2\pi f_k t + \varphi_k\right] \quad (11)$$

where k is the index related with the k-th interharmonic value, K is the value of total interharmonics; b_k represents de values of amplitude of each interharmonic, φ_k represents the values of phase of each interharmonic. f_k represents each interharmonic frequency value.

Interharmonic distortion is included in the form of three frequencies at the 1, 2 and 3 kHz range, which are not correlated to the fundamental frequency as shown in Fig. 3. The numerical values

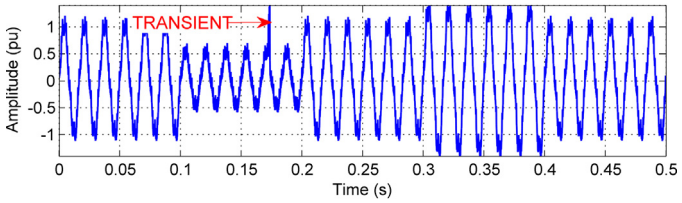

Fig. 4. Fourth step of the construction of a synthetic signal with several PQD: Addition of an oscillatory transient, $x_e(t)$.

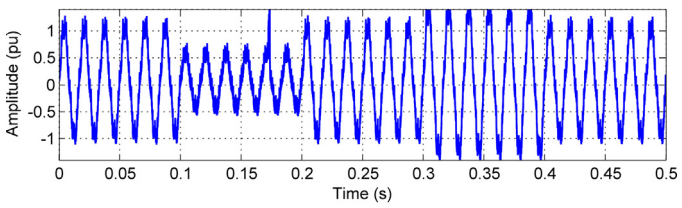

Fig. 5. Final step of the construction of a signal with several PQD: Addition of Gaussian noise, $x_f(t)$.

for interharmonic distortion are set to: $K = 3$; $b_1 = 0.076$; $b_2 = 0.057$; $b_3 = 0.038$; $\varphi_1 = \varphi_2 = \varphi_3 = 0.0$ rads. The interharmonic frequencies, f_k, are set to 1.025, 2.050, and 3.075 kHz.

The fourth step in the method includes an oscillatory transient. Eq. (12) states this new addition to $x_d(t)$.

$$x_e(t) = x_d(t) + \left\{c_m\left[u(t-\alpha_m) - u\left(t-\beta_m\right)\right] \cdot e^{\left[\left(-\frac{t-\alpha_m}{\tau_m}\right)\right]} \cdot \cos\left(2\pi f_m t + \psi_m\right)\right\} \quad (12)$$

where t and $x_d(t)$ is the same that Eq. (10) and Eq. (11) respectively. $u(t)$ is the Heaviside step function, α_m defines the time value when the transient begins, β_m defines the time value when the transient ends. c_m is the amplitude factor for the transient, f_m is the frequency value of the transient, ψ_m is the phase value of the transient. Finally, τ_m is the decay rate value of the transient. The values are set as follows: $\alpha_m = 17.236$ ms; $\beta_m = 17.363$ ms; $f_m = 3$ kHz; $c_m = 0.3$; $\psi_m = 0$ rads; $\tau_m = 1.2728$ ms. Fig. 4 illustrates the resulting waveform $x_e(t)$.

At the fifth and final step, Gaussian noise is added to the resulting waveform of this example, $x_e(t)$. The analytical expression for the final waveform is stated in Eq. (13).

$$x_f(t) = x_e + n(t, x_0, \sigma) \quad (13)$$

The Gaussian noise function is defined by two parameters: a mean value x_0 and its standard deviation σ. For sake of simplicity, the mean value is equal to 0.0 and the standard deviation is set in 0.20. Fig. 5 depicts the final waveform that combines several simultaneous PQD according to the proposed methodology.

The resulting waveform is constructed by using a structured method that is able of generating simultaneous PQD in a single waveform. The resulting waveform can get a different behavior if the parameters of Eq. (6) are adjusted with different numeric values. The method provides a simple and practical way of modeling waveforms with simultaneous PQD similar to those existent in real power systems.

4. Standard definitions of PQD and its modeling

Three waveforms described in international standards are selected in order to assess the capability of the proposed model to reproduce some parametric reference waveforms. The definition of the PQD from each library provides all the information required to tune the proposed model in Eq. (6).

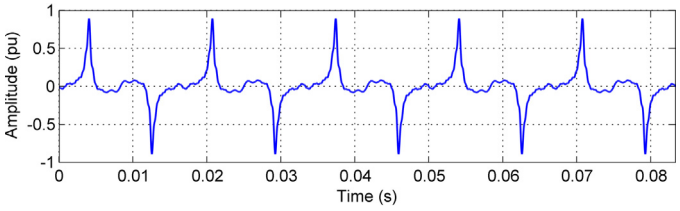

Fig. 6. Time-domain representation of the IEC 61000-3-2 reference harmonic-distorted waveform using the model of Eq. (6).

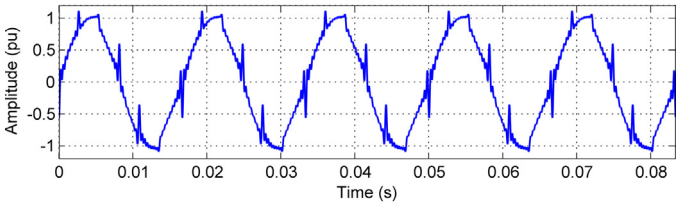

Fig. 7. Time-domain representation of the NRC reference library for a harmonic-distorted waveform using the model of Eq. (6).

4.1. Waveform defined in IEC 61000-3-2 [27]

The international standard IEC 61000-3-2 [27] contains limits for current harmonic emissions and provides a reference library (numerical values) of a fundamental signal with harmonic distortion. This standard provides the amplitude value and phase range for harmonics from the first and up to the 40th harmonic. The total harmonic distortion (TDH index) is about 153.9%.

The proposed model shown in Eq. (6), is tuned exactly using the parameter values indicated in [27] and [32]; the derived expression is shown in Eq. (14). The parameters take the following values: $A = 1.0, f_0 = 60$ Hz, $\theta = 0$ radians, $N = 40$, and finally a_h and θ_h have the numerical values depicted in Table 1. As it can be seen, the waveform defined in IEC 61000-3-2 fits exactly in the proposed model. Fig. 6 shows a time-domain representation of this PQD standard waveform when the model stated in Eq. (6) is adjusted with the parameters defined in [27].

$$x_{IEC}(t) = A \cdot \cos\left[2\pi f_0 t + \theta\right] + \sum_{h=2}^{N} a_h \cos\left[2\pi h f_0 t + \theta_h\right] \tag{14}$$

4.2. NRC proposed waveform

The National Research Council, which is the NMI of Canada, proposed a distorted sinusoidal waveform in [28,29]; specifying amplitude and phase for harmonics from the first and up to the 49th. Eq. (15) is derived from mathematical model in Eq. (6) as described in [33]. The parameter values are: $A = 1.0$, $f_0 = 60$ Hz, $\theta = 0$ radians and $N = 49$. The generated waveform has a THD of 15.4%. Table 2 shows the full set of parameters for the harmonic components a_h and θ_h of the waveform. The waveform originally described in the NRC library is graphically reproduced in Fig. 7 by using the proposed model of Eq. (6), when is adjusted with the parameters shown in [28,29].

$$x_{NRC}(t) = A \cdot \cos\left[2\pi f_0 t + \theta - \frac{\pi}{2}\right] + \sum_{h=2}^{N} a_h \cos\left[2\pi h f_0 t + \theta_h\right] \tag{15}$$

4.3. Flicker waveform used in NPL (UK) for calibration

A flicker event is produced by continuous variations of the supply voltage, non-correlated to the fundamental frequency. Non-correlated phenomena like a flicker, requires well-defined

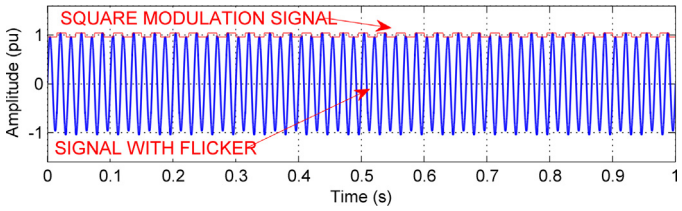

Fig. 8. Time-domain representation using the model of Eq. (6) of the NPL flicker waveform, including the modulation signal.

parameters such as: severity, DV/V, flicker frequency and duration of the event. The National Physical Laboratory, which is the NMI in the UK, proposed a reference waveform used for flicker calibration in [30]. The parameters selected are: flicker frequency 33.33 Hz and DV/V = 2.4 to use in model shown in Eq. (6). Additionally, it is well-known that the flicker is an event of long duration. It is important to notice that the flicker waveform described in [30] is obtained directly from Eq. (6) as stated in Eq. (16)

$$x_{NPL}(t) = A \cdot \left[1 + \delta_a(t)\right] \cdot \left[\cos\left(2\pi f_0 t + \theta\right)\right] \tag{16}$$

where δ_a is a square modulation given by Eq. (17)

$$\delta_a(t) = A_{fl} \cdot sgn\left[\cos\left(2\pi f_{fl} t + \theta_{fl}\right)\right] \tag{17}$$

being A_{fl} the amplitude of a square signal for modulation, directly related to the term DV/V. The function *sgn()* is the well-known sign function. The modulation has a specific frequency of 33.33 Hz, represented by f_{fl}. The modulation phase θ_{fl} has 0 rads. The other parameters take the following values: $A = 1.0$, $f_0 = 60$ Hz, $\theta = 0$ rads. Fig. 8 depicts the time-domain representation of the NPL flicker waveform [30]. The parameters of the waveform are set up exactly as [30].

5. Modeling recorded waveforms

Three different real recorded waveforms are selected in order to compare waveforms obtained from the mathematical model in Eq. (6) with waveform in the literature. The selected waveforms are: (1) a recorded waveform from IEEE used in a workgroup during the development of a published standard [26], (2) a noisy recorded waveform of [26], and (3) a recorded waveform taken from a real power system node.

In each case, it is necessary to perform a previous tuning process for the mathematical model, which means that not all the parameters in Eq. (6) are used simultaneously.

5.1. IEEE recorded waveform wave5.xls from the open library IEEE 1159.2 Working Group [26]

The reference waveform is a recorded waveform of a real PQD from the IEEE 1159.2 working group [26]. This waveform contains 1536 samples of a real PQD event with a sampling frequency of 256 samples per cycle (15.36 kHz). The recorded waveform comprises 6 cycles of the fundamental frequency.

The mathematical model is adjusted using a semi-manual method. The model in Eq. (6) requires numeric values for the parameters that define the model. The method used for identifying the parameters is a traditional spectral analysis based on a *Discrete Fourier Transform* (DFT). The IEEE waveform is separated in 6 sections; each section corresponds to one fundamental cycle of the fundamental. The spectral analysis is made in every one of the six sections; it means that a single DFT is applied in each cycle of the fundamental recorded waveform. At the end of this analysis harmonic content is identified in each cycle of the recorded waveform.

Table 1
Amplitude, a_h, and phase values, θ_h for each harmonic distortion proposed in [27], for $h = 2to40$.

	a_2/θ_2	a_3/θ_3	a_4/θ_4	a_5/θ_5	a_6/θ_6	a_7/θ_7	a_8/θ_8	a_9/θ_9	a_{10}/θ_{10}
	0.4700/0	1.0000/π	0.1870/π	0.4960/0	0.1300/0	0.3350/π	0.1000/π	0.1740/0	0.0800/0
a_{11}/θ_{11}	a_{12}/θ_{12}	a_{13}/θ_{13}	a_{14}/θ_{14}	a_{15}/θ_{15}	a_{16}/θ_{16}	a_{17}/θ_{17}	a_{18}/θ_{18}	a_{19}/θ_{19}	a_{20}/θ_{20}
0.1430/π	0.0667/π	0.0913/0	0.0571/0	0.0652/π	0.0500//π	0.0575/0	0.0444/0	0.0515/π	0.0400/π
a_{21}/θ_{21}	a_{22}/θ_{22}	a_{23}/θ_{23}	a_{24}/θ_{24}	a_{25}/θ_{25}	a_{26}/θ_{26}	a_{27}/θ_{27}	a_{28}/θ_{28}	a_{29}/θ_{29}	a_{30}/θ_{30}
0.0466/0	0.0364/0	0.0425/π	0.0333/π	0.0391/0	0.0308/0	0.0362/π	0.0286/π	0.0337/0	0.0267/0
a_{31}/θ_{31}	a_{32}/θ_{32}	a_{33}/θ_{33}	a_{34}/θ_{34}	a_{35}/θ_{35}	a_{36}/θ_{36}	a_{37}/θ_{37}	a_{38}/θ_{38}	a_{39}/θ_{39}	a_{40}/θ_{40}
0.0316/π	0.0250/π	0.0296/0	0.0235/0	0.0280/π	0.0222/π	0.0264/0	0.0211/0	0.0251/π	0.0200/π

Table 2
Amplitude, a_h, and phase values, θ_h for each harmonic distortion proposed in [33], for h = 2to49.

	a_2/θ_2	a_3/θ_3	a_4/θ_4	a_5/θ_5	a_6/θ_6	a_7/θ_7	a_8/θ_8	a_9/θ_9	a_{10}/θ_{10}
	0.0122/-2.427	0.0212/-2.623	0.0253/-2.775	0.0604/-1.317	0.0246/2.021	0.0153/-0.829	0.0054/-0.684	0.0177/-2.181	0.0222/-2.506
a_{11}/θ_{11}	a_{12}/θ_{12}	a_{13}/θ_{13}	a_{14}/θ_{14}	a_{15}/θ_{15}	a_{16}/θ_{16}	a_{17}/θ_{17}	a_{18}/θ_{18}	a_{19}/θ_{19}	a_{20}/θ_{20}
0.0266/-1.040	0.0272/2.441	0.0128/-1.331	0.0036/0.064	0.0203/-1.956	0.0205/-2.239	0.0153/-0.642	0.0302/2.921	0.0169/-1.083	0.0033/2.401
a_{21}/θ_{21}	a_{22}/θ_{22}	a_{23}/θ_{23}	a_{24}/θ_{24}	a_{25}/θ_{25}	a_{26}/θ_{26}	a_{27}/θ_{27}	a_{28}/θ_{28}	a_{29}/θ_{29}	a_{30}/θ_{30}
0.0235/-1.766	0.0189/-2.110	0.0068/-0.322	0.0331/-2.954	0.0101/-0.754	0.0166/3.014	0.0249/-1.558	0.0166/-2.099	0.0016/-2.750	0.0347/-2.618
a_{31}/θ_{31}	a_{32}/θ_{32}	a_{33}/θ_{33}	a_{34}/θ_{34}	a_{35}/θ_{35}	a_{36}/θ_{36}	a_{37}/θ_{37}	a_{38}/θ_{38}	a_{39}/θ_{39}	a_{40}/θ_{40}
0.0133/-0.396	0.0162/-2.947	0.0242/-1.296	0.0146/-2.178	0.0078/-2.771	0.0344/-2.248	0.0090/0.350	0.0212/-2.534	0.0231/-0.925	0.0170/-2.190
a_{41}/θ_{41}	a_{42}/θ_{42}	a_{43}/θ_{43}	a_{44}/θ_{44}	a_{45}/θ_{45}	a_{46}/θ_{46}	a_{47}/θ_{47}	a_{48}/θ_{48}	a_{49}/θ_{49}	
0.0140/-2.354	0.0354/-1.980	0.0092/1.284	0.0278/-2.274	0.0212/-0.635	0.0225/-2.248	0.0180/-2.176	0.0325/-1.794	0.0113/2.132	

The second stage in the parametric identification corresponds to the evaluation of interharmonic content. The spectral analysis provides an approximation to the values of the interharmonic content, however, the identification of the interharmonic frequencies is made by hand.

If only harmonic and interharmonic content is taken into account for modeling the IEEE waveform according with Eq. (6), there is a difference that evidences that one oscillatory transient is in the original recorded waveform. The identification of the values in the transient event is made by hand when the model approach is compared with the original IEEE waveform, emphasizing on the duration of the transient event and also on the value of the decaying frequency. At this point, acceleration in the fundamental frequency is detected; the model of this acceleration is linear, and also included in the parametric identification.

It is possible to apply the construction method described in Section 2.1 and Section 3 of this paper once the parameters are estimated. The first step is the definition of the fundamental frequency at 60 Hz as shown in Eq. (18).

$$x_\alpha(t) = A \cdot \cos\left[2\pi f_0 t + \theta\right] \tag{18}$$

Where A, f_0, and θ means the same than Eq. (7). The values are $A = 0.58$, $f_0 = 60$ Hz, and $\theta = -0.8726$ rads.

The second step is to set the parameters for the harmonic distortion as stated in Eq. (19).

$$x_\beta(t) = x_\alpha(t) + \sum_{h=2}^{N} a_h \cos\left[2\pi h f_0 t + \theta_h\right] \tag{19}$$

The number of harmonics considered for each cycle are: 25 harmonics for the 1st cycle, 13 harmonics for the 2nd cycle, 100 harmonics for the 3rd cycle and 14 harmonics for the 4th, 5th and 6th cycles. All harmonics contain information of amplitude and phase. For sake of simplicity only the first four parameters for amplitude and phase in each cycle are used for defining Eq. (19) are shown in this paper. Table 3 summarizes the values of amplitude, a_h, and phase, θ_h for each fundamental cycle.

At the third step, an interharmonic non-correlated to the fundamental signal is included, as shown in Eq. (20).

$$x_\gamma(t) = x_\beta(t) + \sum_{k=1}^{K} b_k \cos\left[2\pi f_k t + \varphi_k(t)\right] \tag{20}$$

The function that defines the behavior of the phase of this waveform includes an initial phase and other component related with frequency acceleration. This behavior is approached in Eq. (21):

$$\varphi_k(t) = \varphi_{k0} + \pi t^2 \cdot R_{kf} \tag{21}$$

There are two interharmonic components identified. The values of the parameters in Eq. (20), and in Eq. (21) are: $K = 2$; $b_1 = 0.025$; $b_2 = 0.015$; $f_k = [55\text{ Hz}, 50\text{ Hz}]$; $\varphi_{10} = 0.9948$ rads; $\varphi_{20} = \pi$ rads; $R_{1f} = 103$ Hz/s; $R_{2f} = 205$ Hz/s.

Finally, at the fourth step, a transient PQD is added to the waveform as stated in Eq. (22).

$$x_{IEEE}(t) = x_\gamma(t) + \sum_{m=1}^{M} c_m \left[u(t-\alpha_m) - u\left(t-\beta_m\right)\right] \cdot e\left[\left(-\tfrac{t-\alpha_m}{\tau_m}\right)\right] \cdot \cos\left(2\pi f_m t + \psi_m\right) \tag{22}$$

The parametric vales used in Eq. (22) are: $M = 1$; for $m = 1$ $f_1 = 1.095$ kHz; $c_1 = 0.06354$; $\psi_1 = -\pi$ rad; $\alpha_1 = 45.99$ ms; $\beta_1 = 46.44$ ms, and $\tau_1 = 455$ μs.

Fig. 9 shows the comparison in the time-domain between the recorded waveform and the synthetic waveform constructed with the proposed method. Fig. 10(a) depicts the original waveform from the original recorded library and Fig. 10(b) shows the waveform as synthesized by the model of Eq. (22). Additionally, Fig. 10(c) depicts the difference between the original and the synthetic waveforms, showing that there is a deviation having a mean of 0.26% and a standard deviation of ± 1.01%.

5.2. IEEE recorded waveform wave14a.xls from the open library IEEE 1159.2 Working Group [26]

The second case of study is also a recorded waveform of a real PQD from the IEEE 1159.2 working group [26]. This library contains 1536 samples of a real PQD event with the sampling frequency of 256 samples per cycle (15.36 kHz). The recorded waveform comprises 6 cycles of the fundamental frequency.

The mathematical model is adjusted using a semi-manual method applying the same methodology described in Section 5.1 in this paper. The IEEE waveform is separated into 6 sections; each section corresponding to one fundamental cycle of the fundamental. The spectral analysis is made in every one of the six sections.

Table 3
Values of amplitude and phase for Eq. (19) during each cycle of the fundamental frequency.

Cycle number	a_2/θ_2	a_3/θ_3	a_4/θ_4	a_5/θ_5
1	0.000380/−2.97812	0.007654/0.9973	0.001023/−2.0677	0.009953/−1.8549
2	0.004843/−1.9103	0.005987/−2.7906	0.002352/−0.4409	0.007729/−1.8795
3	0.006032/1.0582	0.012483/2.1829	0.020848/−2.7129	0.019175/−1.8523
4	0.012110/1.3251	0.018599/−3.1367	0.033583/−1.4427	0.006851/−0.6405
5	0.009229/1.2868	0.022149/−3.1362	0.026344/−1.2486	0.012628/−0.5070
6	0.009917/1.4739	0.022153/3.1240	0.024385/−1.2064	0.011017/−0.4135

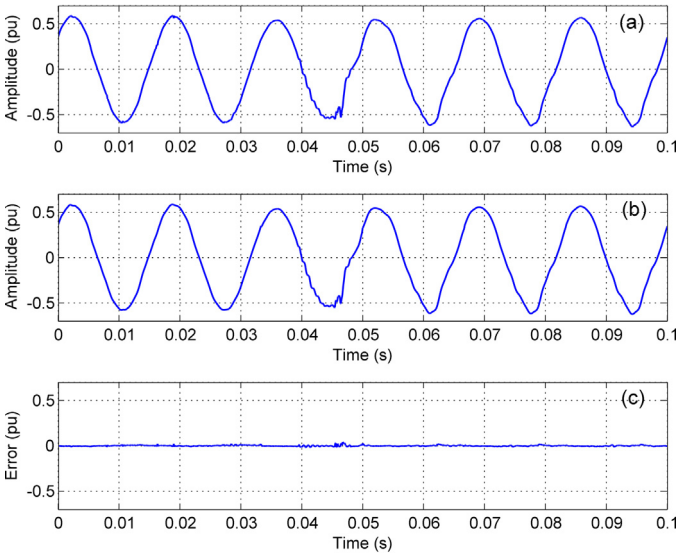

Fig. 9. IEEE 1159.2 recorded waveform: (a) Time-domain recorded waveform, (b) Time-domain model-based waveform, (c) Time-domain difference.

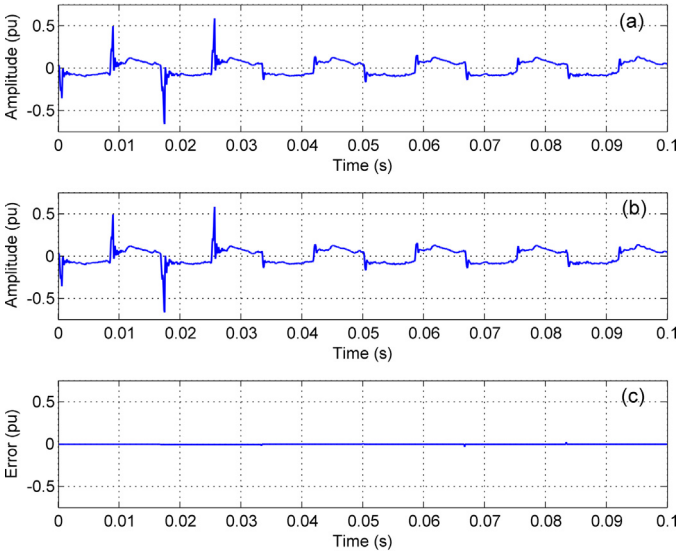

Fig. 10. Real field-recorded waveform case: (a) Time-domain original recorded waveform, (b) Time-domain model-based waveform, (c) Time-domain difference.

The second stage in the parametric identification corresponds to the evaluation of the behavior of the resulting difference between waveforms, the recorded waveform, and the model-based waveform when only harmonic content is added. The resulting behavior is approximated with a Gaussian noise function.

The first step in waveform construction process is the definition of the fundamental frequency at 60 Hz in Eq. (23)

$$x_{\alpha 2}(t) = A \cdot \cos\left[2\pi f_0 t + \theta\right] \tag{23}$$

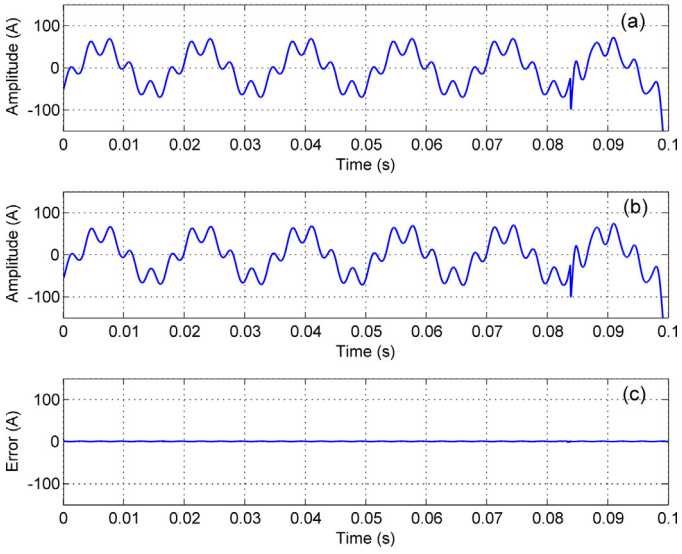

Fig. 11. Real field-recorded waveform case: (a) Time-domain original recorded waveform, (b) Time-domain model-based waveform, (c) Time-domain difference.

where A, f_0, and θ means the same than Eq. (7). The values are $A = 0.1067$, $f_0 = 60$ Hz, and $\theta = 1.6542$ rads.

The second step is to set the parameters for the harmonic distortion as stated in Eq. (24).

$$x_{\beta 2}(t) = x_{\alpha 2}(t) + \sum_{h=2}^{N} a_h \cos\left[2\pi h f_0 t + \theta_h\right] \tag{24}$$

The number of harmonics considered for all cycles are: 128 harmonics. All harmonics contain information of amplitude and phase. For sake of simplicity only the first four harmonic parameters for amplitude and phase are shown in this paper. Table 4 summarizes the estimated values for Eq. (24) in amplitude, a_h, and phase, θ_h.

At the third step, one component related with Gaussian noise is added as stated in Eq. (25).

$$x_{IEEE-2}(t) = x_{\beta 2}(t) + n(t, x_0, \sigma) \tag{25}$$

Where the Gaussian noise function is identified by two parameters: a mean value $x_0 = -0.0017$ and its standard deviation $\sigma = \pm 0.0019$.

Fig. 10 shows the comparison in the time-domain between the recorded waveform and the synthetic waveform constructed with the proposed method. Fig. 11(a) depicts the original recorded waveform from IEEE and Fig. 11(b) shows the waveform as synthesized by the model of Eq. (25). Additionally, Fig. 11(c) depicts the difference between the original and the synthetic waveforms; the error has a mean of 1% and a standard deviation of ± 1%.

5.3. Recorded waveform from a real power system

The waveform of this case of study was recorded during the startup of an arc furnace in a given power system node. The acquisition sampling rate is 15.35 kHz, giving 256 samples per cycle during

Table 4
Values of amplitude and phase for Eq. (24) during each cycle of the fundamental frequency.

Cycle number	a_2/θ_2	a_3/θ_3	a_4/θ_4	a_5/θ_5
1	0.0069/−2.8341,	0.0241/2.0987	0.0053/0.1859	0.0331/1.8674
2	0.0169/−2.9101	0.0459/2.0860	0.0101/1.2406	0.0476/1.7679
3	0.0120/−2.4419	0.0176/1.4400	0.0064/0.1103	0.0183/1.3176
4	0.0138/−2.3459	0.0208/1.4693	0.0076/0.2003	0.0198/1.4036
5	0.0119/−2.6907	0.0198/1.2771	0.0081/0.3893	0.0167/1.2261
6	0.0139/−2.6826	0.0189/1.1945	0.0085/0.5020	0.0167/1.1933

Table 5
Values of amplitude and phase for Eq. (26) during each cycle of the fundamental frequency.

Cycle number	X_{DC}	a_2/θ_2	a_3/θ_3	a_4/θ_4	a_5/θ_5
1	1.7607	0.1417/0.4876	0.2187/2.0398	0.2870/−2.7726	22.5213/−2.0773
2	1.8694	0.0577/1.3622	0.2760/2.5157	0.4031/−1.7170	22.6085/−1.9583
3	1.8694	0.0577/1.3622	0.2760/2.5157	0.4031/−2.7170	22.6085/−1.9583
4	1.8694	0.0577/1.3622	0.2760/2.5157	0.4031/−2.7170	22.6085/−1.9583
5	1.9863	0.1633/−1.2320	0.0600/-2.2736	0.2959/−1.7933	22.4658/−1.9439
6	23.3645	19.3850/−2.7737	15.3887/-2.5223	15.5349/−2.4408	36.1533/−2.0797

100 ms of the testing run using a 16-bit ADC, which comprises 6 cycles of the signal.

In order to identify the parameters of the model in Eq. (6) the process is similar to the cases shown in Sections 5.1, and 5.2. The identification process includes the separation of the recorded waveform in six stages. The first approximation uses the DFT spectral analysis for defining the harmonic content. The second process includes interharmonic content identification. Using the estimates values for harmonic content and for interharmonic content it is possible to reach deviations within 1% of accuracy.

The construction of the mathematical model based on Eq. (6) is developed in three steps.

The first step is the definition of the fundamental frequency at 60 Hz in Eq. (26)

$$x_{\alpha 3}(t) = X_{DC} + A \cdot \cos\left[2\pi f_0 t + \theta\right] \tag{26}$$

where A, f_0, and θ means the same than Eq. (7). The values are $A = 53$, $f_0 = 60$ Hz, and $\theta = -2.421$ rads.

The second step is to set the parameters for the harmonic distortion as stated in Eq. (27).

$$x_{\beta 3}(t) = x_{\alpha 3}(t) + \sum_{h=2}^{N} a_h \cos\left[2\pi h f_0 t + \theta_h\right] \tag{27}$$

The number of harmonics considered for each cycle are: 10 harmonics for the first 5 cycles, whereas 100 harmonics are used for the 6th cycle. All harmonics contain information of amplitude and phase. For sake of simplicity only the first four parameters of amplitude and phase in each cycle are shown in this paper. Table 5 summarizes the values of amplitude, a_h, and phase, θ_h.

The value of the DC component of the recorded waveform is significant compared to the other cases, up to the 5th cycle the value of the DC component is almost constant, for the 6th cycle the DC component increases its value 20 times the original one, it is inferred that the arc furnace started in this cycle.

At the third step, an interharmonic non-correlated to the fundamental signal is included in Eq. (28).

$$x_{\gamma 3}(t) = x_{\beta 3}(t) + b_k \cos\left[2\pi f_k t + \varphi_k\right] \tag{28}$$

There is one interharmonic component identified. The values of the parameters in Eq. (27) are: $b_k = 9$; $f_k = 302$ Hz; $\varphi_k = \pi/4$ rads.

Fig. 11 depicts the comparison in the time-domain between the recorded waveform and the synthetic waveform that it is obtained from the proposed model when using the parameter settings summarized in Table 5. Fig. 11(a) shows the original waveform from the real power system and Fig. 11(b) depicts the waveform as synthesized by the model. Additionally, Fig. 11(c) illustrates the difference between the original and the synthetic waveforms, there is a deviation with a mean of 0.84% and a standard deviation of ± 0.52%.

6. Discussion

The aim of this work is to define a mathematical model that represents different dynamic waveforms, including simultaneous PQD. With the model defined in Eq. (6), it is possible to accurately achieve parametric models that represents physical phenomena in power systems. The methodology developed for constructing waveforms is feasible of being applied in engineering environments just like the electrical utilities.

The proposed model is capable of reproducing waveforms with a minimum error, where the PQD parameters are fully defined. There are well-defined PQD references that can be reproduced as seen in Section 4.1 for the IEC waveform [27], Section 4.2 for the NRC waveform, [28,29]; and Section 4.3 for the NPL flicker waveform, [30]. These standard waveforms are used as PQD references for international standardization, equipment calibration, and for PQ analysis in some National Metrology Institutes worldwide.

When the parameters of the model are not previously known or predefined, like in recorded waveforms, then the model fitting becomes a parameter identification problem. For the cases shown in Sections 5.1–5.3, the chosen methodology for modeling the recorded waveform is to apply classical signal processing techniques in order to estimate the value of the parameters to fit the recorded waveforms into Eq. (6). Once these parameters are estimated, the model is adjusted to reproduce the waveforms. The results show an agreement between the mathematical model and the reference libraries. For those references that provide the exact value of parameters, differences are almost zero. For those recorded waveforms of a given node in a power system, differences are within 1%, which can be further reduced if optimization techniques are used to improve the parameter identification.

The accuracy of this adjustment depends exclusively on how precise the parametric identification process is. In this work the process of identifying parameters is made by spectral analysis in combination with a semi-manual analysis of the behavior of differences between the recorded waveforms and the model-based waveform. This last parametric identification relays directly on the expertise of the authors. The accuracy of the model is related to the process of selecting and identifying the whole set of different PQD and their parameters that a given recorded waveform contains. The computational burden is almost negligible because the

semi-manual process is made in a post-processing stage, the computational resources are not critical due the fact that one part of the identification of parameters relays on classic processing techniques, *i.e.* DFT. The other part of the parameter identification relays directly on the expertise of the user. The aim of this work is focused in provide a mathematical model capable of representing multiple simultaneous PQD. Using the proposed model and the constructing methodology, it is possible to reproduce waveforms from standards and also from recorded waveforms in power systems. The identification process of parameters in this work is aimed to explore the capability of the proposed model to be fitted in different scenarios and not as an optimal solution for parametric identification in waveforms.

If the accuracy is a key feature when PQ waveforms are modeled, then an automatic method is required for parametric identification. There are efforts in that direction, for instance in [34], a method based on micro-genetic algorithms for detecting and classifying electric power disturbances is addressed. The method proposed in this reference is capable of detecting and classifying several PQD at one single step automatically. In this work, some PQD cases are explored such as: sag events, swell, unbalance, among other amplitude related disturbances. The methodology proposed in [34] can be extended to different PQD if these events can be parameterized into a mathematical model taking into account the advantages of the micro-genetic algorithms. The scheme proposed in [34] achieves results within 5% of accuracy with reduced computational resources when these resources are compared to other approaches.

The proposed method for modeling waveforms is prepared for dynamic cases where the parameters are either time variant or completely non-periodic. It is possible to expand the model to waveforms that may contain dynamic PQD such as: simultaneous modulation of amplitude and phase, fluctuant harmonics, interharmonics near to the value of the fundamental frequency, for behavior related to non-linear electrical loads, for dynamic off-nominal conditions in islanding conditions, and so on, even in the case when the acquisition of the waveforms is subject to noise in non-clearly repetitive patterns. When real waveforms are recorded, it is possible that they contain non-periodic patterns; in that case, the proposed mathematical model is able of responding to this challenges if the constructing process for any waveform is applied as shown in this paper, and even more important, if the fitting process is developed using more sophisticated analysis tools in order to accurately estimating the parameters in the model. The model considers a section for non-correlated components with not-Gaussian nature; this section is able to be extended to those patterns and disturbances.

Even for cases where no periodic noise is added into the acquiring systems. In this last dynamic cases, the complexity for the identification process grows while the identification process is semi-manual, in fact it is expected a more complex identification process when the fitting process include time variant or non-periodic behaviors in the waveforms.

7. Conclusions

The proposed methodology is capable of adjusting a mathematical model aiming to represent various types of PQD, when the parameters of a given waveform are known *a priori;* and also when the waveform is obtained from a real recorded sampled signal. This represents a key feature of the proposed model if it is used in PQ analysis applications. The proposed methodology is broadly inclusive due to the way it can reproduce a wide number of simultaneous PQD from a single analytical expression. This model is a generalization of the major models already in use for PQD and PQ analysis.

Three different sets of results are obtained. First, it is demonstrated the step-by-step construction of a synthetic waveform with several simultaneous PQD. Then, the model is used to reproduce waveforms defined in standard libraries from the parameter definition of the PQD described in those libraries. The model is adjusted to reproduce recorded waveforms from real power systems. In the case of recorded waveforms, an additional problem of parameter identification arises, requiring further development of optimization techniques for improving the parameter identification to better fit those waveforms into the proposed model. Future work includes the development of these automatic tools oriented to optimize the parameters of the proposed model to fit recorded waveforms and minimizing the resultant error.

Acknowledgements

The authors would like to thank to the Centro Nacional de Metrología (CENAM), Mexico, for providing the facilities to develop this research work and to the program SIDEPRO of CENAM for their invaluable support.

References

[1] V.V. de Araujo, R. Acosta-Hernandez, E. Simas, A. de Oliveira, W.L.A. de Oliveira, Dedicated hardware implementation of a high precision power quality meter, 2015 IEEE International Instrumentation and Measurement Technology Conference (I2MTC) (2015) 393–398.
[2] M. Valtierra-Rodriguez, R.J. Romero-Troncoso, R.A. Osornio-Rios, A. Garcia-Perez, Detection and classification of single and combined power quality disturbances using neural networks, IEEE Trans. Ind. Electron. 61 (5) (2014) 2473–2482.
[3] D. Granados-Lieberman, R.J. Romero-Troncoso, R.A. Osornio-Rios, A. Garcia-Perez, E. Cabal-Yepez, Techniques and methodologies for power quality analysis and disturbances classification in power systems: a review, IET Gener. Transm. Dis. 5 (4) (2011) 519–529.
[4] Electromagnetic compatibility (EMC) – Part 4–7: Testing and measurement techniques – General guide on harmonics and interharmonics measurements and instrumentation, for power supply systems and equipment connected thereto, IEC 61000-4-7 (2002).
[5] Electromagnetic compatibility (EMC) – Part 4–11: Testing and measurement techniques – Voltage dips, short interruptions and voltage variations immunity tests, IEC 61000-4-11 (2004).
[6] Electromagnetic compatibility (EMC) – Part 4–15: Testing and measurement techniques – Flickermeter – Functional and design specifications, IEC 61000-4-15 (2010).
[7] Electromagnetic compatibility (EMC) – Part 4–30: Testing and measurement techniques – Power quality measurement methods, IEC 61000-4-30 (2015).
[8] Voltage characteristics of electricity supplied by public distributions systems, BS EN 50160 (2000).
[9] P. Thakur, A.K. Singh, Unbalance voltage sag fault-type characterization algorithm for recorded waveform, IEEE Trans. Power Deliv. 28 (2) (2013) 1007–1014.
[10] M.R. Alam, K.M. Muttaqi, A. Bouzerdoum, A new approach for classification and characterization of voltage dips and swells using 3-D polarization ellipse parameters, IEEE Trans. Power Deliv. 30 (3) (2015) 1344–1353.
[11] G.A. Kyriazis, P.M. Ramos, A. Cruz-Serra, Bayesian and least-squares algorithms for estimating signal harmonics: a comparative study, Elsevier Meas. 45 (9) (2012) 2203–2212.
[12] D. Belega, D. Dallet, D. Slepicka, Accurate amplitude estimation of harmonic components of incoherently sampled signals in the frequency domain, IEEE Trans. Instrum. Meas. 59 (5) (2010) 1158–1166.
[13] C. Matthews, P. Clarkson, P.M. Harris, W.G.K. Ihlenfeld, P.S. Wright, Evaluation of flicker measurement uncertainties by a Monte Carlo method, IEEE Trans. Instrum. Meas. 60 (7) (2011) 2255–2261.
[14] M.H.J. Bollen, I.Y.H. Gu, Origin of power quality variations, in: Signal Processing of Power Quality Disturbances, 1st ed., IEEE Press, John Wiley & Sons Inc., New York, 2006, pp. 41–161.
[15] A.J. Arana, J.N. Bank, R.M. Gardner, L. Yil, Estimating speed of frequency disturbance propagation through transmission and distribution systems, PSCE '06. 2006 IEEE PES Power Systems Conference and Exposition (2006) 1286–1290.
[16] N. Nimpitiwan, G. Heydt, R. Ayyanar, J. Blevins, K. Koellner, K. Kittredge, M. Chandler, The propagation of disturbances in power distribution systems, 2003 IEEE PES Transmission and Distribution Conference and Exposition (2003).
[17] T. Radil, P.M. Ramos, F.M. Janeiro, A. Cruz Serra, PQ monitoring system for real-time detection and classification of disturbances in a single-phase power system, IEEE Trans. Instrum. Meas. 57 (8) (2008) 1725–1733.
[18] P.K. Dash, K.B. Panigrahi, D.K. Sahoo, G. Panda, Power quality disturbance data compression, detection, and classification using integrated spline wavelet and S-transform, IEEE Trans. Power Deliv. 18 (2) (2003) 595–600.

[19] C. Muscas, Power quality monitoring in modern electric distribution systems, IEEE Instrum. Meas. Mag. 13 (5) (2010) 19–27.
[20] Y. Huang, Y. Liu, Z. Hong, Detection and location of power quality disturbances based on mathematical morphology and hilbert-huang transform, 9th International Conference on Electronic Measurement & Instruments 2009. ICEMI '09 (2009) 2-319–2-324.
[21] D. Granados-Lieberman, M. Valtierra-Rodriguez, L. Morales-Hernandez, R.J. Romero-Troncoso, R.A. Osornio-Rios, A Hilbert transform-based smart sensor for detection, classification, and quantification or power quality disturbances, Sensors 13 (2013) 5507–5527.
[22] M. Kezunovic, A. Yuan Liao, A novel software implementation concept for power quality study, IEEE Trans. Power Deliv. 17 (2) (2002) 544–549.
[23] A.J. Roscoe, I.F. Abdulhadi, G.M. Burt, P and M class phasor measurement unit algorithms using adaptive cascaded filters, IEEE Trans. Power Deliv. 28 (3) (2013) 1447–1459.
[24] S. Khokhar, A.A. Mohd Zin, A.S. Mokhtar, N. Ismail, MATLAB/Simulink based modeling and simulation of power quality disturbances, 2014 IEEE Conference on Energy Conversion (CENCON) (2014) 445–450.
[25] A. Pavas, H. Torres-Saínchez, A. Delgadillo, A novel approach for the simulation of power quality stationary disturbances in electric power systems, 2010 14th International Conference on in Harmonics and Quality of Power (ICHQP) (2010) 1–9.
[26] IEEE 1159.2 Working Group, Test waveforms, wave5. xls. [Online]. Available: grouper.ieee.org/groups/1159/2/testwave.html.
[27] IEC 61000-3-2, Electromagnetic compatibility (EMC) – Part 3-2: Limits – Limits for harmonic current emissions (equipment input current ≤16 A per phase).
[28] R. Arseneau, P. Filipski, A calibration system for evaluating the performance of harmonic power analyzers, IEEE Trans. Power Deliv. 10 (3) (1995) 1177–1182.
[29] R. Arseneau, P. Filipski, An efficient test method for harmonic measurement equipment, Proceedings. 8th International Conference on in Harmonics and Quality of Power Proceedings (1998) 233–237.
[30] NPL Power Quality Waveform Library, 'flicker waveforms', available on-line: http://resource.npl.co.uk/waveform/datafiles/flicker_waveform_library.pdf (accessed on august 2015).
[31] S. Herraiz-Jaramillo, G.T. Heydt, E. O'Neill-Carrillo, Power quality indices for aperiodic voltages and currents, IEEE Trans. Power Deliv. 15 (2) (2000) 784–790.
[32] Fluke Multifunction Calibrator 5520A PQ Opt. Service Manual, Table 9. 7–8, available on line: http://us.flukecal.com/products/obsolete-products/5520a-high-performance-multi-product-calibrators-0?quicktabs_product_details=4#quicktabs_product_details (2001).
[33] Fluke Multifunction Calibrator 5520A PQ Opt. Service Manual, Table 12. 11-12, available on line: http://us.flukecal.com/products/obsolete-products/5520a-high-performance-multi-product-calibrators-0?quicktabs_product_details=4#quicktabs_product_details (2001).
[34] A.Y. Jaen-Cuellar, L. Morales-Vazquez, R.J. Romero-Troncoso, D. Moriñigo-Sotelo, R.A. Osornio-Rios, Micro-genetic algorithms for detecting and classifying electric power disturbances, Neural Comput. Appl. (2016), http://dx.doi.org/10.1007/s00521-016-2355-z.